Combined Participation of Hydroxylase Active Site Residues and Effector Protein Binding in a *Para* to *Ortho* Modulation of Toluene 4-Monooxygenase Regiospecificity†

Kevin H. Mitchell, Joey M. Studts, and Brian G. Fox*

Department of Biochemistry, College of Agricultural and Life Sciences, University of Wisconsin, Madison, Wisconsin 53706-1544

Received November 8, 2001; Revised Manuscript Received January 10, 2002

ABSTRACT: Toluene 4-monooxygenase (T4MO) is a diiron hydroxylase that exhibits high regiospecificity for *para* hydroxylation. This fidelity provides the basis for an assessment of the interplay between active site residues and protein complex formation in producing an essential biological outcome. The function of the T4MO catalytic complex (hydroxylase, T4moH, and effector protein T4moD) is evaluated with respect to effector protein concentration, the presence of T4MO electron-transfer components (Rieske ferredoxin, T4moC, and NADH oxidoreductase), and use of mutated T4moH isoforms with different hydroxylation regiospecificities. Steady-state kinetic analyses indicate that T4moC and T4moD form complexes of similar affinity with T4moH. At low T4moD concentrations, the steady-state hydroxylation rate is linearly dependent on T4moD−T4moH complex formation, whereas regiospecificity and the coupling efficiency between NADH consumption and hydroxylation are associated with intrinsic properties of the T4moD−T4moH complex. The optimized complex gives both efficient coupling and high regiospecificity with *p*-cresol representing >96% of total products from toluene. Similar coupling and regiospecificity for *para* hydroxylation are obtained with T3buV (an effector protein from a toluene 3-monooxygenase), demonstrating that effector protein binding does not uniquely determine or alter the regiospecificity of toluene hydroxylation. The omission of T4moD causes an ∼20-fold decrease in hydroxylation rate, nearly complete uncoupling, and a decrease in regiospecificity so that *p*-cresol represents ∼60% of total products. Similar shifts in regiospecificity are observed in oxidations of alternative substrates in the absense or upon the partial removal of either T4moD or T3buV from toluene oxidations. The mutated T4moH isoforms studied have apparent V_{max}/K_M specificities differing by ∼2−4-fold and coupling efficiencies ranging from 88% to 95%, indicating comparable catalytic function, but also exhibit unique regiospecificity patterns for all substrates tested, suggesting unique substrate binding preferences within the active site. The G103L isoform has enhanced selectivity for *ortho* hydroxylation with all substrates tested except nitrobenzene, which gives only *m*-nitrophenol. The regiospecificity of the G103L isoform is comparable to that observed from naturally occurring variants of the toluene/benzene/*o*-xylene monooxygenase subfamily. Evolutionary and mechanistic implications of these findings are considered.

The soluble diiron hydroxylases are an evolutionarily related family of enzymes that includes the methane (*2*−*6*), toluene (*7*−*11*), benzene (*12*), and *o*-xylene (*13*) monooxygenases, phenol hydroxylases (*14*), and alkene epoxidases (*15*−*18*). All of these complexes consist of an electron-transfer chain (either an FAD- and [2Fe-2S]-containing NADH oxidoreductase or an oxidoreductase and a Rieske-type [2Fe-2S] ferredoxin), a catalytic effector protein containing neither organic cofactors nor metal ions, and a terminal hydroxylase. The hydroxylases have an $(\alpha\beta\gamma)_2$ quaternary structure with typical $M_r \approx 200-250$ kDa with a diiron center contained in each α-subunit. Single turnover (*4*, *7*, *9*) and peroxide shunt catalysis (*19*−*21*) have established that the diiron center of the hydroxylase component is the minimal requirement for the chemical reaction. Moreover, transient kinetic (*22*) and spectroscopic studies (*23*) of MMO[1] have shown that an O_2 adduct named compound O, diferric peroxo species named compound P* and compound P, and a high-valent species named compound

† This work was supported by the National Science Foundation Early Career Development Program (MCB-9733734) and the Petroleum Research Fund (32955-AC4) to B.G.F. K.H.M. was a trainee of the NIH Institutional Biotechnology Pre-Doctoral Training Grant T32 GM08349. J.M.S. was supported in part by a Peterson/Wharton Fellowship from the Department of Biochemistry, University of Wisconsin.

* Corresponding author: Enzyme Institute Building, Room 146, 1710 University Ave., University of Wisconsin, Madison, WI 53705. Phone: (608) 262-9708. Fax: (608) 265-2904. E-mail: bgfox@biochem.wisc.edu.

[1] Abbreviations: T4MO, four-protein toluene 4-monooxygenase complex from *Pseudomonas mendocina* KR1; T4moH, hydroxylase component of T4MO; T4moC, Rieske [2Fe-2S] ferredoxin component of T4MO; T4moD, catalytic effector component of T4MO; T4moF, NADH:ferredoxin oxidoreductase component of T4MO; MMO, methane monooxygenase; MmoB, effector protein of MMO; MmoH, hydroxylase component of MMO; MmoR, reductase component of MMO; T3buV, catalytic effector component of the toluene 3-monooxygenase from *Pseudomonas pickettii* PKO1.

10.1021/bi012036p CCC: $22.00
Published on Web 02/02/2002

Q successively appear as intermediates during the reaction cycle (*24*−*34*). Compound Q is kinetically competent in the hydroxylation of methane (*22*) and norcarane (*35*), whereas compound P has been found to be independently capable of olefin epoxidation (*30*).

The presently available data, which also derives largely from catalytic, spectroscopic, and structural characterizations of MMO, show that a ternary complex of MmoB, MmoR, and MmoH is relevant to catalysis (*36*, *37*). Complex formation between MmoB and MmoH provides a remarkable variety of influences on the catalytic cycle, such as modulating the diiron center redox potentials and electron-transfer rates (*38*), promoting the coupling between the redox equivalents consumed and the yield of product (*2*, *4*), altering the regiospecificity of reaction with nonphysiological substrates (*20*), changing the rates of formation and disappearance of reaction cycle intermediates P and Q (*34*), and controlling the access/egress of large substrates to the active site (*34*). These catalytic enhancements are thought to arise from binding-induced conformational changes. The likelihood of these changes is also supported by changes in spectroscopic properties of the diiron center upon complex formation (*36*, *39*) and by X-ray scattering studies that showed dramatic changes in the overall shape and size of the complex (*37*). MmoR also participates in the regulation of catalysis by causing shifts in the redox potentials of the diiron center that favor $2e^-$ transfer and by increasing the rate of reaction between the diferrous MmoH−MmoB complex and O_2 (*40*−*42*).

Less detail is available regarding the role of protein complex formation in the reactions of other members of the diiron hydroxylase family. One relevant area of inquiry involves the role of protein−protein interactions in controlling regiospecificity with substrates such as toluene that can give rise to multiple products (*13*, *43*). Moreover, the commonality of the influences that the effector protein and electron-transfer components may have on the diiron center reactivity when a compound of lower thermodynamic stability than methane is the physiologically relevant substrate has not been addressed in other members of this family.

The present work focuses on T4MO, a diiron hydroxylase that catalyzes the NADH- and O_2-dependent hydroxylation of toluene to form *p*-cresol (*9*). This four-component complex consists of an NADH oxidoreductase (T4moF, 33 kDa), a Rieske-type ferredoxin (T4moC, 12.5 kDa), an effector protein (T4moD, 11.6 kDa), and a diiron hydroxylase [T4moH, with a $(\alpha\beta\gamma)_2$ quaternary structure, 212 kDa]. T4MO is a member of the toluene/benzene monooxygenase branch of the diiron hydroxylase phylogenetic tree (*44*). This enzyme exhibits a high regiospecificity for *para* hydroxylation in the reaction with toluene (*45*) and in reactions with a wide variety of other nonphysiological, singly substituted aromatic compounds (*45*−*47*). This high fidelity provides the basis for an assessment of the interplay between T4moD and T4moH in producing an essential biological outcome.

Here, the function of the T4MO complex has been evaluated using varied amounts of T4moD and T3buV [the effector protein from a putative toluene 3-monooxygenase complex (*44*, *48*)], the electron-transfer components, and mutated T4moH isoforms exhibiting inherently different patterns of hydroxylation regiospecificity. The T201A isoform has been previously shown to provide partial changes in regiospecificity for toluene hydroxylation and V_{max}/K_M in steady state comparable with the natural isoform (*46*); the G103L isoform introduced here was created on the basis of primary sequence alignments with other toluene, phenol, and alkene monooxygenases. The analysis of the changes in rate, coupling, and regiospecificity shows that effector protein binding provides an essential enhancement of catalytic rate, while coupling and regiospecificity arise as intrinsic properties of the T4moH isoform in the complex. In this evaluation, the T4moH active site provides the primary constraints responsible for the regiospecificities characteristic of the natural, the artificially engineered, and the heterologously reconstituted enzyme complexes.

MATERIALS AND METHODS

Materials. Enzyme substrates and products and other chemicals were from Aldrich (Milwaukee, WI). *N*-Methyl-*N*-(trimethylsilyl)trifluoroacetamide was from Pierce (Rockford, IL). Vent DNA polymerase and restriction enzymes were from New England Biolabs (Beverly, MA). DNA extraction and purification kits were from Q-BIO (Carlsbad, CA) and Qiagen (Valencia, CA). *Escherichia coli* strains DH5α (Pharmacia, Piscataway, NJ) and BL21(DE3) (Novagen, Madison, WI) were used for cloning and expression, respectively. PCR primers were from Integrated DNA Technologies, Inc. (Coralville, IA). Methods and overall strategies for PCR amplification, and the protocols used to express and purify the T4MO proteins, including the T201G and G103L isoforms and T3buV, were as previously described (*11*, *44*−*46*). A unit of T4MO activity is defined as the formation of 1 μmol of *p*-cresol/min in air-saturated 50 mM phosphate buffer, pH 7.5 at 298 K, in the presence of optimal concentrations of the T4MO components, toluene-saturated buffer (5.8 mM at 298 K), and NADH (0.5 mM).

G103L Isoform of T4moH. The G103L isoform was constructed by overlap extension PCR using the T4moH expression vector pKM10 as the template, Vent DNA polymerase, and a Perkin-Elmer Model 9600 thermocycler (Perkin-Elmer, Foster City, CA) (*46*). The following oligonucleotide sequences were used as primers: ABEF3 (5′-atgcttccggctcgtatgttgtgtgg-3′), G103LF (5′-gccatcgcagtt-CTGgaatatgcagc-3′), G103LR (5′-gctgcatattcCAGaactgc-gatggc-3′), and ENDR (5′-cgaccccaacgtttattccatcctgg-3′). Capital letters indicate the nucleotide changes that gave the G103L mutation. To generate the products for the initial overlap extension PCR, a 50 μL reaction was subjected to 30 cycles of melt at 94 °C for 30 s, anneal at 58 °C for 30 s, and extend at 72 °C for 45 s. These PCR products were gel-purified and used in a second overlap extension PCR consisting of 12 cycles of primerless PCR in a 100 μL reaction using 6 μL of each gel-purified product from the initial overlap extension PCR as template. After the 12 cycles, the primers ABEF3 and ENDR were added for an additional 18 cycles to enhance amplification of the complete 1266 bp fragment. The 30 cycles consisted of melt at 94 °C for 45 s, anneal at 58 °C for 45 s, and extend at 72 °C for 45 s. The final PCR product was digested with *Eco*RI and *Bgl*II and cloned into the vector pKM10 for sequence analysis and protein overexpression as described previously (*11*). The DNA encoding the G103L isoform was sequenced using the Big Dye sequencing kit (Perkin-Elmer) at the University of Wisconsin Biotechnology Center.

Product Distributions. Enzyme reactions were performed in Teflon-sealed 5 mL reaction vials in a total volume of 250 μL of 50 mM potassium phosphate buffer, pH 7.5, in a reciprocating water bath at 26 °C and 250 rpm. An optimized reaction contained 2 nmol each of T4moC and T4moD and 0.2 nmol of T4moF for each nanomole of T4moH protomer present. As indicated, T4moD was either decreased, omitted, or substituted with T3buV in other reactions. Substrates were added using a gastight syringe, and the enzyme reaction was initiated with the addition of 0.5 μmol of NADH. After the appropriate time, aliquots of the enzyme reactions were removed and quenched by rapid injection into a 0.4 mL centrifuge tube containing 100 μL of chloroform and 50 μL of 0.1 M HCl saturated with NaCl. The quenched reaction was vigorously mixed for 15 s and then separated by centrifugation (14000*g* for 2 min). The organic layer from the extraction (typically 2 μL) was used for product analyses. An internal calibration standard of 3-methylbenzyl alcohol (25 μM) was included in the chloroform.

Product distributions were determined by gas chromatography using a Hewlett-Packard 6890 gas chromatograph equipped with a 7683 autoinjector and either a BP20 column (30 m × 0.25 mm, 0.25 μm film thickness; SGE, Austin, TX) for the toluene and methoxybenzene oxidation products or an EC-1 column (30 m × 0.25 mm, 0.25 μm film thickness; Alltech Associates, Inc., Deerfield, IL) for chlorobenzene and nitrobenzene oxidation products. The columns were connected to flame ionization detectors. The injector and detector were maintained at 250 °C, and a split ratio of 0.5:1 was used. The He carrier flow rate for the BP20 column was maintained at 4.0 mL/min, while the He flow rate for the EC-1 column was maintained at 3.0 mL/min for separation of the chlorophenolic products and 4.2 mL/min for separation of the nitrophenolic products. Retention times were determined by comparisons to neat standards.

For the toluene oxidation products, the following temperature program was used: 100−130 °C at a rate of 5 °C/min; 130−144 °C at 2 °C/min; 144−200 °C at 30 °C/min; 200 °C for 7 min. Under these conditions, benzyl alcohol and *o*-, *p*-, and *m*-cresols eluted at 7.1, 9.8, 11.8, and 12.0 min, respectively. The internal standard 3-methylbenzyl alcohol eluted at 9.0 min. For the methoxybenzene oxidation products, the following temeperature program was used: 100−130 °C at 5 °C/min; 130−150 °C at 2 °C/min; hold at 150 °C for 9 min; 150−200 °C at 5 °C/min; hold at 200 °C for 7.5 min. Under these conditions, 2-methoxyphenol, phenol, 4-methoxyphenol, and 3-methoxyphenol eluted at 7.0, 10.2, 24.2, and 26.6 min, respectively, while the internal standard 3-methylbenzyl alcohol eluted at 9.0 min.

Products from the chlorobenzene and nitrobenzene oxidations were derivatized with *N*-methyl-*N*-(trimethylsilyl)trifluoroacetamide prior to chromatographic analyses. For the derivatized chlorobenzene oxidation products, the following temperature program was used: 70 °C for 1 min; 70−75 °C at 2 °C/min; 75 °C for 1 min; 75−120 °C at 4 °C/min; 120 °C for 2 min; 120−200 °C at 30 °C/min; 200 °C for 6 min. Under these conditions, the 2-, 3-, and 4-chlorophenol isomers eluted at 15.6, 16.1, and 16.7 min, respectively, while the internal standard 3-methylbenzyl alcohol eluted at 16.9 min. For the derivatized nitrobenzene oxidation products, the following temperature program was used: 125−150 °C at 2 °C/min; 30 °C/min to 240 °C; 240 °C for 10 min. Under these conditions, *o*-, *p*-, and *m*-nitrophenol eluted at 6.2, 7.2, and 9.0 min, respectively, while the internal standard 3-methylbenzyl alcohol eluted at 3.6 min.

Coupling Determinations, O_2 Polarography, and NADH Regeneration System. Coupling efficiency is defined as the percentage of the moles of total hydroxylated products recovered per mole of NADH utilized. Coupling was determined using optical spectrometry, O_2 polarography, and gas chromatography as previously described (*9*). Catalase and superoxide dismutase (Sigma Chemical Co., St. Louis, MO) were dissolved in 50 mM buffer, pH 7.5, and added to the reaction mixtures when indicated (200−4000 and 10 units, respectively) in order to diminish the accumulation of either H_2O_2 or O_2^- from uncoupled NADH utilization. An NADH generation system (*49*) consisting of NADH (0.5 μM), glucose 6-phosphate, and glucose-6-phosphate dehydrogenase was investigated as indicated.

Kinetic Analyses. For steady-state kinetic analysis of protein complex formation, each individual protein component was treated as a substrate, while all other protein components of the T4MO complex, O_2, toluene, and NADH were maintained at saturating levels. Enzyme reactions were performed in Teflon-sealed 5 mL reaction vials in a total volume of 250 μL of 50 mM potassium phosphate buffer, pH 7.5, in a reciprocating water bath at 26 °C and 250 rpm. An optimized reaction contained 2 nmol each of T4moC and T4moD and 0.2 nmol of T4moF for each nanomole of T4moH protomer present. The O_2 concentration was that of an air-saturated buffer solution. Control experiments showed that NADH, O_2, and toluene were not limiting during these reactions. Rates were determined by linear least-squares fitting of the time dependence of product formation as determined by gas chromatography (*50*); K_M values were determined by linear least-squares fitting of the time dependence of NADH utilization as determined by optical spectroscopy under conditions giving maximal coupling. For T4moF and T4moC, the velocity data were fit to the Michaelis−Menten equation, $v = V_{max}[S]/(K_M + [S])$, where V_{max} is the apparent maximal reaction velocity, [S] is the concentration of the varied protein component, and K_M is the apparent Michaelis constant for the varied protein component. For T4moD (*44*), the velocity data were fit to an equation accounting for the formation of both activating and inhibiting complexes of the effector protein, $v = V_{max}[S]/(K_M + [S] + ([S]^2/K_I))$, where the additional term K_I is the equilibrium constant for formation of an inhibiting complex containing the effector protein. The kinetic parameters and error estimates were determined using the statistically weighted nonlinear least-squares fitting routines HYPERO and SUBINO (*51*). Apparent V_{max} and K_M values for different substrates were determined with optimal protein concentration as previously described (*46*, *52*). In all cases, apparent V_{max} values are reported as turnover numbers relative to the concentration of ($\alpha\beta\gamma$) protomer of T4moH.

For studies of the effect of low concentrations of T4moD on catalysis, the rate, coupling, and regiospecificity values were normalized for comparison by examining fractional changes. For example, the fractional change in rate, *f*, was defined as $[1 - (V_{max} - v_i)/(V_{max} - v_{min})]$, where V_{max} is the maximal velocity for the enzyme reaction obtained at the optimal concentration ofT4moD, v_i is the rate observed at a given concentration of T4moD, and v_{min} is the rate observed

Table 1: Survey of Product Distributions and Total Products Obtained from Toluene Oxidation by Different T4MO Complexes

complex[b]	catalase[c]	product distribution[a]				total products
		p-cresol	*o*-cresol	*m*-cresol	benzyl alcohol	
complete	no	1857 (96.6)	17 (0.9)	35 (1.8)	13 (0.7)	1922
−T4moD, −T4moH	no	nd[d]	nd	nd	1 (100)	1[e]
−T4moD	no	9 (54.3)	3 (16.7)	1 (6.8)	4 (22.2)	16
−T4moD	yes	30 (62.5)	8 (16.7)	3 (5.6)	7 (15.3)	49
−T4moD, +NADH regeneration	no	8 (50.0)	2 (16.0)	1 (6.0)	4 (28.0)	15
−T4moD, +NADH regeneration	yes	26 (50.2)	8 (15.3)	3 (5.4)	15 (29.1)	52
0.05 nmol of T4moC/protomer	yes	28 (86.3)	1 (2.2)	1 (2.1)	3 (9.4)	160
−T4moF, +FdR, +NADPH	yes	211 (93.6)	2 (1.0)	5 (2.1)	7 (3.3)	225

[a] Nanomoles of product recovered after 5 min from single experiments to illustrate changes in product distribution from the various enzyme complexes. Percentages of total products are shown in parentheses. For the complete enzyme complex, similar percentages have been reported elsewhere (*45*−*47*). [b] Reaction mixtures and NADH regeneration system as described in Materials and Methods. Changes in reaction constituents are indicated. [c] Presence or absence of 4000 units of catalase. [d] nd, not detected at the detection limit of 0.1 nmol. [e] See footnote 2.

without T4moD. Fractional changes in coupling and regiospecificity were calculated in an analogous manner.

RESULTS

Performance of the Reconstituted T4MO Complex. Table 1 shows that reconstitution of the T4MO complex with the complete, optimal composition of protein components gave the maximal total yield of products and a high regiospecificity for *p*-cresol formation. Omission of both T4moD and T4moH from the reaction gave no products.[2] For the T4MO complex lacking T4moD, an ∼97% decrease in the total amount of hydroxylated products was observed even as a fixed amount of NADH was completely consumed over an extended time period. Furthermore, as elaborated below, the regiospecificity for *p*-cresol formation was compromised in the absence of T4moD. The addition of catalase (4000 units) to reactions lacking T4moD increased the total product yield by ∼3-fold (Table 1), presumably by protecting one or more of the proteins of the complex from H_2O_2-mediated inactivation. Consequently, catalase was added to all reactions, particularly those containing either substoichiometric amounts of T4moD or mutated T4moH isoforms in order to maximize product yields. The use of a regeneration system to maintain NADH levels gave no significant improvement in product yields but did lead to changes in the product distribution primarily associated with an increase in the percentage of benzyl alcohol (Table 1). Since this increase may arise from adventitious metal-catalyzed oxidations (*53*), the NADH generation system was not used in the remaining studies of this work.

Effect of T4moD on Reaction Rate. T4moD (*44*) and other diiron hydroxylase effector proteins (*36*, *40*, *42*) form activating and inhibitory complexes. T4moD has an apparent $V_{max} = 3.4 \pm 0.5\ s^{-1}$ and apparent $K_M = 2.0 \pm 0.6\ \mu M$ for the activating complex (*44*) and an apparent K_I value of $28 \pm 10\ \mu M$. The apparent V_{max} value determined for T4moD is consistent with the steady-state turnover rate of the complete T4MO complex as determined with respect to T4moH. Table 2 shows that removal of T4moD from the enzyme complex caused a decrease in the rate of toluene hydroxylation. In Figure 1, the fractional change in turnover rate (squares) is plotted versus the concentration of T4moD present. In the concentration range shown, corresponding to the linear region of the T4moD saturation binding curve, [T4moD] $\ll K_M$ and $v = (V_{max}/K_M)[E]_0[S]$, with $[E]_0$ corresponding to the fixed amount of [T4moH] present in the assay and [S] corresponding to varied [T4moD]. The solid line in Figure 1 was calculated from this velocity expression using the V_{max} and K_M values for T4moD reported above and by evaluating [T4moH] and [T4moD] according to the appropriate experimental conditions. The goodness of fit (r^2 value of 0.998, confirming that these data were obtained in the second-order region for enzyme catalysis) indicated that T4moD was the rate-limiting constituent added to the steady-state enzyme reaction. Furthermore, this concentration dependence established that T4moD directly participated in the enhancement of catalytic rate. Thus a T4moD−T4moH complex is an essential element of T4MO catalysis.

Table 3 shows turnover rates obtained with T4moH and mutated isoforms with alternative substrates. These nonsubstituted and singly substituted aromatic substrates were compatible with the overall hydrophobic nature of the T4moH active site and also provided a range of substituent electronic effects due to the identity of the ring substituent (*54*). Methoxybenzene and toluene were most rapidly oxidized, whereas chlorobenzene and nitrobenzene were more slowly oxidized. For this group of substrates, a plot of $\log[k_{cat}/k_{benzene}] = \rho\sigma_p^+$ gave $\rho < 0$, indicating the reaction was hindered by electron-withdrawing substituents (*54*). These observations are consistent with electrophilic aromatic substitution and the generation of a carbocationic intermediate providing the framework for the mechanism of the T4moH reaction with aromatic substrates.

Effect of T4moD on Coupling Efficiency. Table 2 and Figure 1 show the effect of changes in T4moD concentration on the coupling efficiency. Unlike the fractional change in rate observed at low concentrations of T4moD, Figure 1 shows that the fractional change in coupling efficiency (circles) was essentially independent of [T4moD] until this concentration was decreased to values that gave 20% or less of the maximal rate. Below this ratio, the coupling changed linearly between the maximal and minimal values (the dashed line of Figure 1 is derived from linear least-squares fitting of the linear region of the T4moD concentration curve; for comparison a simple hyperbolic fit to the regiospecificity and coupling data is shown as the dotted line of Figure 1).

[2] Toluene contained a trace-level contamination of benzyl alcohol. Examination of the time dependence of changes in the product distributions during a 1−5 min reaction revealed that the proportion of *p*-, *o*-, and *m*-cresols increased linearly from nondetectable amounts throughout the entire time period whereas the proportion of benzyl alcohol increased linearly from the initial amount of trace contamination.

Table 2: Influence of T4moD on Rate, Coupling, and Products of Toluene 4-Monooxygenase Oxidation Reactions

substrate	effector protein[a] (μM)	ratio[b]	rate[c] (s^{-1})	coupling[d]	product distribution[e]							
					p-cresol	*m*-cresol	*o*-cresol	benzyl alcohol	*p*-OH	*m*-OH	*o*-OH	cyclo-hexanol
toluene	T4moD											
	40	2.0	2.8	98	96.9 (0.4)	1.6 (0.2)	0.9 (0.1)	0.7 (0.2)				
	10	0.5	2.5	91	96.7 (0.2)	1.5 (0.2)	1.0 (0.1)	0.9 (0.3)				
	4	0.2	1.3	85	95.4 (0.7)	1.6 (0.3)	1.5 (0.5)	1.5 (0.6)				
	2	0.1	0.76	87	93.2 (1.9)	1.9 (0.2)	2.5 (0.9)	2.4 (1.0)				
	1	0.05	0.42	63	88.5 (3.3)	2.3 (0.1)	4.9 (2.0)	4.2 (1.3)				
	0	0	0.13	4	63.3 (1.7)	4.8 (1.2)	16.7 (0.6)	15.2 (1.2)				
	T3buV											
	40	2.0	2.0	>90	95.5 (0.5)	2.7 (0.2)	1.2 (0.1)	0.8 (0.2)				
	10	0.5			95.7 (0.1)	2.6 (0.1)	1.2 (0.1)	0.5 (0.1)				
	2	0.1			92.7 (0.1)	2.9 (0.1)	2.6 (0.1)	1.9 (0.1)				
	1	0.05			89.7 (0.5)	3.2 (0.1)	4.1 (0.4)	3.0 (0.1)				
nitrobenzene	T4moD											
	40	2.0	0.13	65					91.6 (0.7)	8.4 (0.7)	nd[f]	
	10	0.5	0.07						91.2 (0.2)	8.8 (0.2)	nd	
	4	0.2	0.02						87.5 (0.9)	12.6 (0.9)	nd	
	1	0.1	nd									
	0	0	nd									
cyclohexane	T4moD											
	40	2.0	0.13	3								100
	0	0	0.01									100

[a] The enzyme complex was reconstituted as in Table 1 with the concentration of either T4moD or T3buV varied as indicated. [b] Molar ratio of T4moD relative to T4moH protomer present. [c] Turnover number relative to T4moH protomer as calculated from the sum of all products identified by gas chromatography. [d] Percentage of nanomoles of total products relative to nanomoles of NADH utilized. Blank entries were not determined. [e] Percentage of total products recovered after complete utilization of NADH. For experiments with T4moD, standard deviations observed from 3 < *n* < 10 individual determinations are shown in parentheses; for T3buV, the standard deviation was from two experiments. [f] nd, not detected.

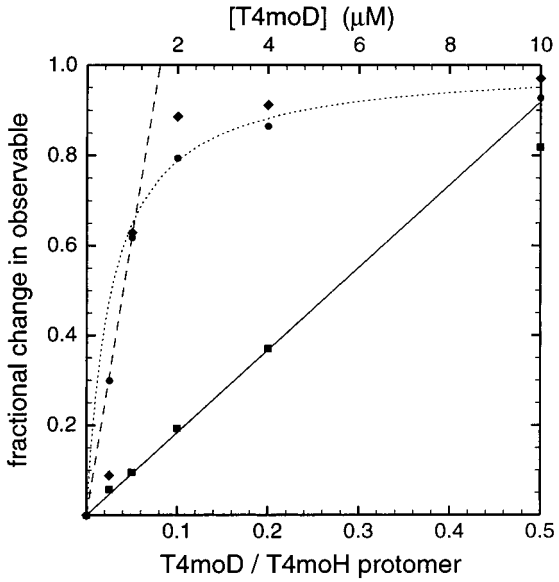

FIGURE 1: Fractional change in rate, coupling, and regiospecificity of the T4MO complex reconstituted with a varied concentration of T4moD relative to T4moH. Key: turnover rate (■); coupling (●); regiospecificity (◆). Lines were calculated using the binding models and fitting procedures as described in Materials and Methods.

The complete removal of T4moD from the complex caused a nearly complete loss of coupling so that only ~4% of the NADH consumed gave rise to hydroxylated products. In this uncoupled state, O_2^- and H_2O_2 were detected. As discussed below, it is most likely that these uncoupling products arose from independent reactions of the electron-transfer proteins.

Effect of T4moD on Regiospecificity. Table 2 and Figure 1 show that complete removal of T4moD caused a partial loss in the high regiospecificity for *p*-cresol formation characteristic of the complete T4MO complex. The control

Table 3: Turnover Numbers for Alternative Substrates by T4moH Isoforms[a]

substrate	σ^+ value[b]	isoform		
		T201 rate (s^{-1})	T201G rate (s^{-1})	G103L rate (s^{-1})
methoxybenzene	−0.780	1.6 (0.1)	3.6 (0.8)	1.2 (0.3)
toluene	−0.310	2.8 (0.2)	3.1 (0.5)	1.9 (0.1)
benzene		0.6 (0.1)	1.9 (0.3)	0.9 (0.2)
chlorobenzene	0.115	1.7 (0.1)	0.9 (0.1)	0.8 (0.1)
nitrobenzene	0.790	0.2 (0.1)	0.1 (0.1)	0.05 (0.0)

[a] Maximal rate (k_{cat}) for total product formation observed for the indicated T4moH isoform in the presence of a saturated aqueous solution of the indicated substrate, NADH, and other protein components as described in Materials and Methods. Standard deviation in rates calculated from 3 < *n* < 10 individual determinations. [b] σ_p^+ values for electrophilic aromatic substitution involving carbocationic intermediates from ref *54*.

experiments of Table 1 indicated that these changes were associated with T4moH-catalyzed reactions since no cresol products and only a small amount of benzyl alcohol[2] were observed in the absence of T4moH. As described above for the coupling efficiency, and also distinct from the result obtained for fractional changes in rate, Figure 1 shows that the fractional change in regiospecificity (diamonds) for *p*-cresol formation did not substantially shift until the amount of T4moD relative to T4moH protomer was decreased to small values.

Figure 1 (solid line) shows that an increase in the T4MO catalytic rate corresponds to the concentration-dependent formation of a complex between T4moD and T4moH. In contrast, coupling and regiospecificity appear to maximize independently in a different concentration regime of T4moD (Figure 1, dashed line), suggesting that these catalytic properties arise from intrinsic features of an already formed T4moD−T4moH complex.

Table 4: Apparent Kinetic Parameters of T4moH Isoforms for Toluene Oxidation[a]

isoform	V_{max} (s^{-1})	K_M (μM)	V_{max}/K_M ($s^{-1}\,\mu M^{-1}$)	coupling efficiency (%)
T201	2.8	4	0.7	98
T201G	3.0	9	0.3	88
G103L	1.8	9	0.2	81

[a] Determined using a complete T4MO complex reconstituted with the indicated T4moH isoform as described in Materials and Methods. V_{max} values are based on total hydroxylation products.

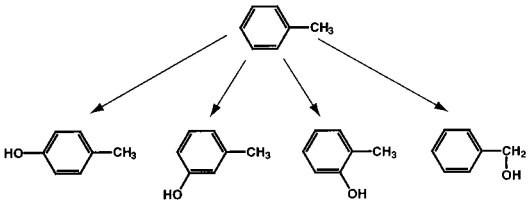

	A	B	C	D
with T4moD				
T201	96.6 (0.4)	1.8 (0.2)	0.9 (0.1)	0.7 (0.2)
T201G	94.3 (0.4)	0.1 (0.1)	4.5 (0.1)	1.1 (0.4)
G103L	24.4 (0.1)	19.7 (0.2)	55.4 (0.2)	0.5 (0.1)
without T4moD				
T201	63.2 (0.7)	5.5 (0.1)	16.5 (0.3)	14.8 (0.5)
T201G	29.6 (0.3)	2.2 (0.1)	56.7 (0.2)	11.5 (0.3)
G103L	5.6 (0.1)	13.3 (0.3)	77.4 (0.3)	3.7 (0.4)
with T3buV				
T201	95.5 (0.5)	2.7 (0.2)	1.2 (0.1)	0.8 (0.2)
G103L	24.4 (0.1)	21.3 (0.2)	54.3 (0.3)	n.d.

FIGURE 2: Product distributions observed during the hydroxylation of toluene by T4moH and the T201G and G103L isoforms in either the presence or absence of T4moD or the presence of T3buV. All reactions were performed in the presence of catalase as described in Materials and Methods. For experiments with T4moD, standard deviations observed from $3 < n < 10$ individual determinations are shown in parentheses; for T3buV, the standard deviation was from two experiments. n.d., not detected.

Table 2 also summarizes the role of T4moD in the T4MO-catalyzed oxidations of nitrobenzene and cyclohexane. Both of these substrates were oxidized by T4MO in the presence of stoichiometric quantities of T4moD, albeit with rates ~20-fold slower than that observed for toluene oxidation. As T4moD was removed from reactions containing nitrobenzene as the substrate, the product distribution underwent a shift toward the electronically favored *m*-nitrophenol. At [T4moD] equivalent to where the regiospecificity of toluene oxidation was noticeably diminished, nitrobenzene oxidation was not observed. Small amounts of cyclohexanol were obtained from reactions with cyclohexane either in the presence or in the absence of T4moD. Since no cyclohexanol was observed in reactions lacking T4moH, and since the addition of catalase did not change the yield, cyclohexanol apparently represents the product of a poor substrate of T4moH. In the presence of T4moD, the oxidation of both nitrobenzene and cyclohexane was substantially uncoupled (Table 2). No further investigation of the origin of the decreases in coupling efficiency upon removal of T4moD was undertaken with these substrates.

Role of the T4moH Active Site in Determining Regiospecificity. Table 4 compares the kinetic parameters obtained from the oxidation of toluene by T4moH and two mutated isoforms. The T201G isoform was described in a previous study (*46*); the G103L isoform has been introduced in this work. These isoforms have apparent V_{max} and K_M values and coupling efficiencies for toluene oxidation comparable to those of the natural enzyme, demonstrating that each is an effective catalyst of aromatic hydroxylation. The comparability of V_{max} values also extends to reactions with the alternative substrates (Table 3). However, Figures 2−5 show that these isoforms give distinct product distributions for toluene and the alternative substrates, supporting the conclusion that the T4moH active site residues provide a major determinant of hydroxylation regiospecificity (*45*, *46*).

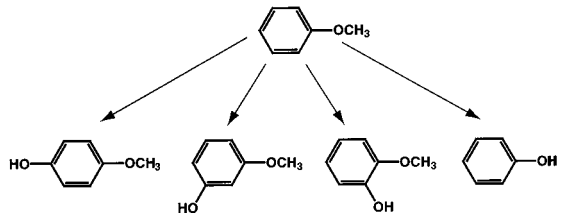

	A	B	C	D
with T4moD				
T201	98.1 (0.2)	0.4 (0.1)	1.4 (0.1)	n.d.
T201G	96.9 (0.2)	n.d.	3.1 (0.2)	n.d.
G103L	73.3 (0.6)	3.8 (0.3)	21.6 (0.1)	1.2 (0.1)
without T4moD				
T201	71.7 (1.0)	n.d.	26.2 (1.3)	2.1 (0.9)
T201G	37.4 (0.5)	n.d.	62.6 (0.5)	n.d.
G103L	24.0 (1.3)	1.0 (0.6)	75.0 (1.0)	n.d.

FIGURE 3: Product distributions observed during the hydroxylation of methoxybenzene by T4moH and the T201G and G103L isoforms in either the presence or absence of T4moD. Other details as in Figure 2.

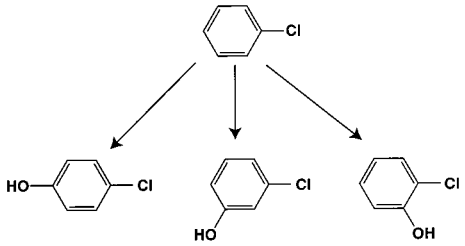

	A	B	C
with T4moD			
T201	97.9 (0.3)	1.7 (0.3)	0.4 (0.1)
T201G	93.8 (1.5)	1.5 (0.3)	4.7 (1.2)
G103L	39.5 (1.2)	38.3 (0.4)	22.2 (0.9)
without T4moD			
T201	86.4 (0.3)	4.9 (0.2)	8.7 (0.3)
T201G	44.5 (2.6)	2.4 (0.1)	53.1 (2.7)
G103L	20.5 (0.1)	13.8 (0.1)	65.6 (0.1)

FIGURE 4: Product distributions observed during the hydroxylation of chlorobenzene by T4moH and the T201G and G103L isoforms in either the presence or absence of T4moD. Other details as in Figure 2.

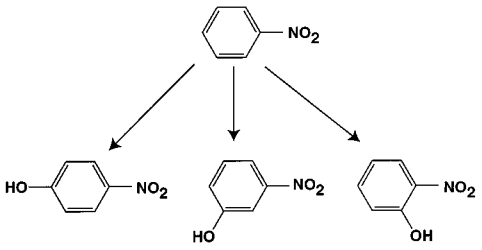

	A	B	C
with T4moD			
T201	91.6 (0.7)	8.4 (0.7)	n.d.
T201G	81.9 (1.9)	10.2 (0.4)	7.9 (2.0)
G103L	3.6 (0.4)	96.4 (0.9)	n.d.
with T3buV			
T201	90.1 (0.2)	9.9 (0.2)	n.d.
G103L	7.4 (0.2)	92.6 (0.2)	n.d.

FIGURE 5: Product distributions observed during the hydroxylation of nitrobenzene by T4moH and the T201G and G103L isoforms in the presence of T4moD. No oxidation of nitrobenzene was observed in the absence of T4moD. Other details as in Figure 2.

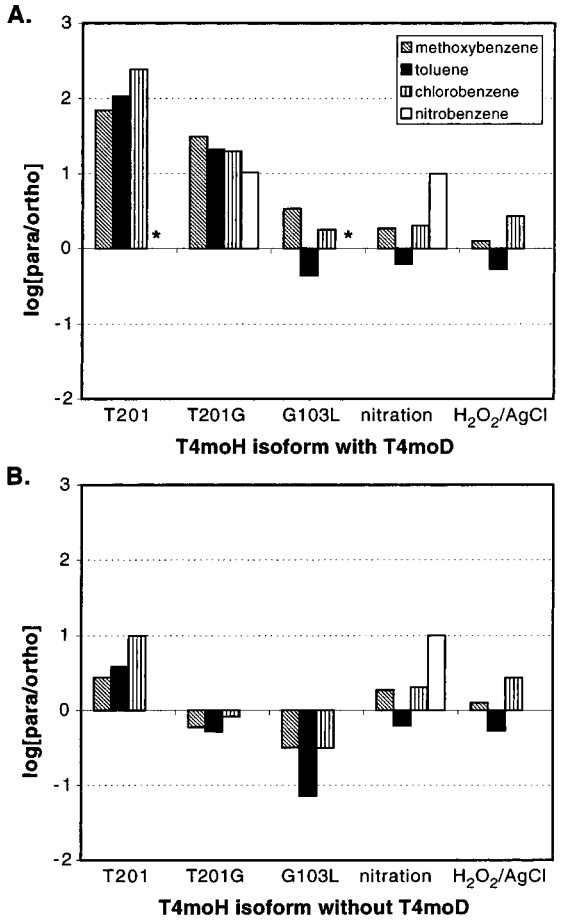

FIGURE 6: Comparison of the *para* to *ortho* ratios for (left to right) toluene, methoxybenzene, chlorobenzene, and nitrobenzene given by the indicated T4moH isoforms, nitration in fuming nitric acid (*90*), or H_2O_2-dependent hydroxylation in the presence of $AgCl_2$ (*91*). A log scale is used on the *y*-axes of (A) and (B) for clarity because of the $\sim 10^4$-fold differences observed; substrates are marked as indicated in the inset to (A). (A) *Para* to *ortho* ratio in the presence of T4moD. No *ortho* product was detected from nitrobenzene by reactants marked with an asterisk. (B) *Para* to *ortho* ratio observed in the absence of T4moD. Nitrobenzene was not oxidized by any T4moH isoform in the absence of T4moD.

The *para/ortho* ratios given by the T4moH isoforms are compared with results obtained from two different solution reactions in Figure 6. A log scale is used for the *y*-axes because of the $\sim 10^4$-fold difference in the ratios obtained for these various experimental systems. When T4moD was included in the T4MO complex, both the natural and the T201G isoforms retained overall high regiospecificity for *para* hydroxylation with all substrates examined (Figure 6A). In contrast, the G103L isoform had an apparently increased regiospecificity for *ortho* hydroxylation with methoxybenzene, toluene, and chlorobenzene in the presence of T4moD (as demonstrated by a decrease in the *para/ortho* ratio). Moreover, the G103L isoform gave only *m*-nitrophenol (Figure 5) from the oxidation of nitrobenzene and elevated percentages of *meta*-hydroxylation products for each of the other substrates investigated. Comparison of panels A and B of Figure 6 showed that removal of T4moD from the reconstituted enzyme complex caused a decrease in the *para/ortho* ratio for all isoforms. This change was most apparent with the G103L isoform, where the ratio of *para/ortho* products (Figure 6B) markedly shifted in favor of *ortho* hydroxylation when compared to the product distributions observed from either the natural isoform or the solution-catalyzed electrophilic aromatic substitution reactions. The differences in product distributions of the enzyme and solution reactions indicate that steric interactions within the active site of the G103L isoform continue to influence the outcome of the reaction, even in the absence of T4moD. Moreover, these interactions lead to an enhanced preference for *ortho* hydroxylation.

No isoform (including the natural enzyme, Figure 5) was capable of nitrobenzene hydroxylation in the absence of T4moD. Since hydroxylation of nitrobenzene is predicted to be the most difficult reaction examined on the basis of electronic considerations (*54*), the oxidizing capability of T4moH may be diminished by removal of T4moD.

Substitution of Other Effector Proteins. A previous study of catalytic cross-reactivity showed that T3buV was able to substitute for the closely related T4moD in reconstitution of the T4MO complex (*44*), while the more distantly related T2bmC and S1 [effector proteins of the *Pseudomonas* species JS150 toluene 2-monooxygenase (*8*) and the *Burkeholderia cepacia* G4 toluene 2-monooxygenase/2-methylphenol 6-hydroxylase (*7*), respectively] were unable to substitute for T4moD. A V_{max}/K_M comparison for T4moD and T3buV showed only an ~2-fold preference for T4moD. Thus T3buV provides ~70% of the V_{max} value obtained from T4moD at optimal concentrations, suggesting that these two effector proteins have overall compatible biological functions. In light of this catalytic competence, the ability of T3buV to alter the regiospecificity of T4moH-catalyzed reactions was tested. Table 2 and Figure 2 show that reconstitution of the T4moH complex with T3buV gave a regiospecificity for toluene hydroxylation that was indistinguishable from the regiospecificity obtained by reconstitution with T4moD. Moreover, a similar partial loss of regiospecificity was observed as T3buV was removed from the heterologous reconstitution reactions (Table 2). The complex of T3buV and the G103L isoform of T4moH gave a product distribution for toluene that again matched that observed from the complex of T4moD with the G103L isoform within experimental error (Figure 2). Furthermore, the regiospecificity of nitrobenzene oxidation obtained from the T3buV−T4moH complex was likewise indistinguishable from that of the T4moD−T4moH complex and yielded *p*-nitrophenol as the major product (Figure 5). These results indicate that effector protein binding does not uniquely control the regiospecificity of T4MO monooxygenation. In contrast, we conclude that the architecture of the T4moH active site provides the primary determinants for regiospecificity of toluene oxidation, with T4moD binding providing an incremental refinement leading to the desired biological outcome. Possible origins of this incremental refinement are considered in the Discussion.

Electron-Transfer Components. Figure 7A shows the changes in reaction velocity observed as the concentration of either T4moC or T4moF was varied relative to fixed concentrations of T4moH and the other components. The lines were generated by nonlinear least-squares fitting using the Michaelis−Menten equation as described in Materials and Methods.

The data of Figure 7A provide an apparent $V_{max} = 3.6 \pm 0.2\ s^{-1}$ and apparent $K_M = 2.1 \pm 0.3\ \mu M$ for T4moC and an apparent $V_{max} = 3.3 \pm 0.2\ s^{-1}$ and apparent $K_M = 0.14 \pm$

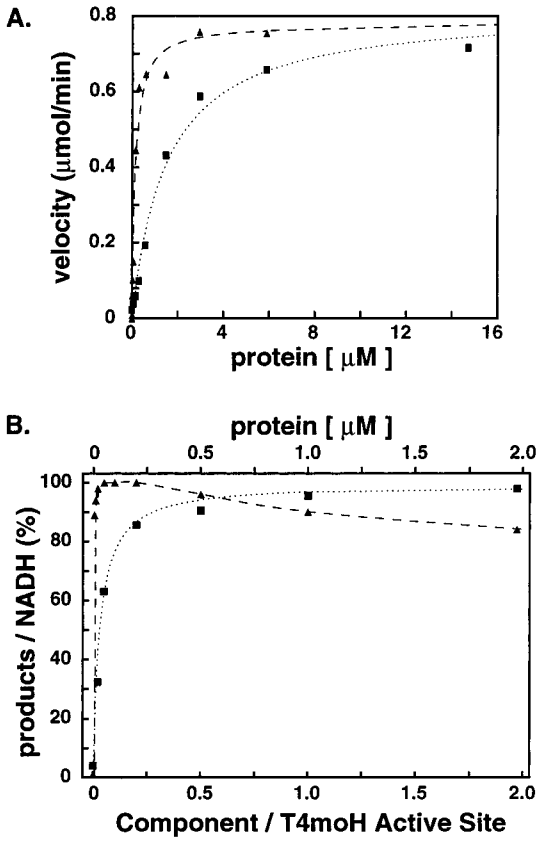

FIGURE 7: Effect of varied concentrations of either T4moC (■, dotted line) or T4moF (▲, dashed line) on the reconstituted T4MO complex: (A) reaction velocity; (B) coupling efficiency. Lines were calculated using the binding models and nonlinear least-squares fitting as described in Materials and Methods.

0.03 μM for T4moF. An inhibitory complex comparable to that formed from T4moD (*44*) was not observed from either T4moC or T4moF. The apparent V_{max} values determined for the two T4MO electron-transfer components are equivalent and consistent with the steady-state turnover rate determined with respect to either T4moH or T4moD. Moreover, the apparent K_M value for T4moC closely matched that determined for T4moD, suggesting that these proteins may contribute to the same catalytic complex. In contrast, the apparent K_M value for T4moF was ~15-fold lower than that determined for either T4moC or T4moF, suggesting that T4moF may be involved in the formation of a different complex, possibly involving T4moC and T4moF only. As reported previously, no hydroxylation was observed in the absence of either T4moC or T4moF (*9*). However, T4moF could be substituted by corn root ferredoxin in reconstitution assays containing T4moC (Table 1), showing that a specific electron-transfer complex involving T4moF was not required for catalysis by the T4MO complex.

Figure 7B shows the change in coupling efficiency as an individual electron-transfer protein was varied relative to a fixed amount of T4moH and the other two components. For T4moC, an ~2:1 ratio with the T4moH protomer gave the highest level of coupling (>90%). The coupling efficiency for T4moC decreased slightly as the ratio of T4moC per T4moH protomer was increased, with ~45% coupling observed at a molar ratio of 20:1 (data not shown). Reaction of T4moC with O_2 in the same concentrations used for reconstitution of the complete enzyme complex (with the NADH-dependent reduction catalyzed by low concentrations of T4moF) gave primarily O_2^- (>90% yield relative to total NADH consumed) with an apparent formation rate (~30 nmol/min) that was only ~4-fold slower than the toluene hydroxylation reaction catalyzed by the complete complex. The predominance of O_2^- as an uncoupling product is consistent with the $1e^-$ reactivity of a reduced [2Fe-2S] center in T4moC with O_2. For T4moF, a molar ratio of ~0.1 T4moF per T4moH protomer gave the optimal coupling (Figure 7B) as well as the maximal rate for *p*-cresol formation (Figure 7A). Further increases in the amount of T4moF (Figure 7B) to an equimolar or higher ratio relative to T4moH caused a noticeable reduction in coupling efficiency. Reaction of T4moF alone with NADH in aerobic buffer gave a mixture of both O_2^- (80%) and H_2O_2 (20%) with an apparent total formation rate (~10 nmol/min) that was ~12-fold slower than the rate of the toluene hydroxylation reaction catalyzed by the complete complex. The detection of both O_2^- and H_2O_2 from the uncoupled reaction of T4moF is consistent with known reactivities of the iron−sulfur and FAD cofactors present in this component (*55*, *56*).

Reactions where the concentrations of both T4moF and T4moC were decreased by 20-fold relative to an equimolar mixture of T4moH and T4moD gave no change in the regiospecificity for toluene hydroxylation (Table 1). A 20-fold decrease of T4moC alone relative to fixed, optimal amounts of T4moH, T4moD, and T4moF gave no change in regiospecificity but an ~10-fold decrease in the rate of product formation. Likewise, substitution of T4moF with corn root ferredoxin reductase gave no change in the regiospecificity for toluene oxidation (Table 1) other than a small increase in benzyl alcohol yield likely due to uncoupled reactions.

DISCUSSION

The diiron hydroxylase enzyme family has been naturally diversified for the oxidation of a variety of different substrates (*57*−*59*). Each of these structurally related complexes initiates a bacterial metabolic pathway allowing the target hydrocarbon to be used as the sole source of carbon and energy. As compared to the three-component MMO complex, T4MO consists of four protein components. This difference introduces questions regarding the degree to which the roles and functions of the effector and electron-transfer proteins will be maintained, particularly when a compound of lower thermodynamic stability than methane is the biological substrate.

Electron-Transfer Proteins. In typical assay concentrations, the rates for autoxidation of either T4moF alone or the combination of T4moF and T4moC in aerobic buffers were ~5−10-fold slower than the rate of toluene hydroxylation in the presence of an optimized ratio of T4moH and T4moD. This difference undoubtedly contributes to the coupling efficiency of the reconstituted four-protein complex. T4moF provided both the maximum rate for *p*-cresol formation and the optimal coupling at substoichiometric quantities. Since T4moF could be substituted by other oxidoreductases including corn root ferredoxin NADPH oxidoreductase (Table 1 and ref *9*) and endogenous *E. coli* reductases (*60*), the primary function of T4moF may be to maintain T4moC in the reduced state as opposed to forming a discrete, essential

catalytic complex with T4moH. By this assessment, the apparent role of T4moF is more limited than those assigned to MmoR, which participates in the regulation of MMO catalysis in a number of ways (*20*, *41*, *42*).

Previous studies have shown that T4moC is required for steady-state catalysis (*9*). Here, T4moC was shown to provide maximal reaction rates and high coupling efficiency when present in approximately stoichiometric quantities relative to T4moH. Moreover, the steady-state kinetic results (Figures 1 and 7) indicate that T4moC and T4moD both form complexes of similar affinity with T4moH, perhaps representing a catalytically relevant ternary complex. However, since T4moC is an obligate $1e^-$ carrier, two discrete electron-transfer events (and possibly two binding complexes) will likely be required in order to satisfy the monooxygenase stoichiometry of the T4MO reaction. Other diiron enzymes (e.g., toluene 3-monooxygenase, benzene monooxygenase, plant acyl-ACP desaturase) also use ferredoxin as an intermediate electron donor, underscoring the importance of this electron-transfer chain configuration and stoichiometry to the diversity of diiron enzyme function. The participation of ferredoxin as an intermediate donor represents another distinction with MMO, where one ternary complex between reduced MmoR and resting MmoH can give $2e^-$ transfer. Whether T4moC binding provides additional inputs to T4MO catalysis related to those identified for MmoR binding in MMO catalysis remains an open question. However, a 20-fold change in the concentration of T4moC relative to the other enzyme components or the substitution of T4moF by another oxidoreductase gave no changes in regiospecificity for toluene oxidation (Table 1), suggesting that the T4MO electron-transfer components do not directly participate in this aspect of catalysis.

The results show that both T4moC and T4moF yield reduced O_2 products (i.e., O_2^- or H_2O_2) that could, in principle, yield adventitious oxidations or other deleterious outcomes. Uncoupling of the electron-transfer chain has been inferred to have an adverse influence on bacterial cell growth rates and volumetric productivity during expression of recombinant T4MO (*11*). For reactions such as methane hydroxylation or fatty acid desaturation, adventitious oxidations would either be energetically infeasible or be easily recognized by an incorrect regio- or stereochemistry. In contrast, for substrates that offer the possibility of more complex product distributions (such as toluene), or for more easily oxidized substrate analogues that might be used for certain types of mechanistic studies, this recognition may be more difficult. Therefore, we considered the possibility that adventitious oxidations may contribute to the product distributions. The increase in benzyl alcohol yield observed when NAD(P)H-regeneration systems were used (Table 1) suggests that the use of this method to increase the yield of products from slow substrates or to enhance the performance of catalytically compromised mutated isoforms should be undertaken with caution.

Effector Protein. The present studies have used recombinant T4MO proteins individually produced in different *E. coli* hosts, which allows reconstitution of the enzyme complex without the possibility for trace-level contamination from an incomplete purification. This overcame a limitation of our initial characterizations of the role of T4moD in catalysis (*9*), which could not be successfully removed from the original T4moH preparations without inactivation of the latter. In the present work, increases in catalytic rate were shown to correspond to the concentration-dependent formation of a complex between T4moD and T4moH (Figure 1, solid line). In contrast, coupling and regiospecificity maximized in a different concentration regime of T4moD, suggesting that these catalytic properties arise from intrinsic features of an already formed T4moD−T4moH complex. In overview, these results correspond to the known properties of MmoB, supporting the evolutionary relationship of both effector protein and diiron hydroxylase components.

One functional comparison between MmoB and T4moD is that MmoB binding gives an ∼150-fold increase in the turnover rate for methane (*4*, *36*), a difficult to oxidize aliphatic hydrocarbon that can yield only one relevant physiological product. For comparison, T4moD binding gives a relatively smaller ∼20-fold rate enhancement in the turnover rate for toluene (Table 2) but refines the distribution of four possible product isomers to give the physiologically relevant *p*-cresol as the only significant product.

In the absence of detailed structural characterizations of the interactions between T4moD and T4moH, changes in catalytic rate, coupling, and regiospecificity are currently best rationalized in terms of binding-induced conformational change. The carboxylate shifts observed in X-ray structures (*61*−*65*) and the changes in spectroscopic properties (*28*, *36*, *38*, *39*, *66*−*73*) and X-ray scattering characteristics (*37*) observed in other diiron enzymes offer indications of the ways that protein binding interactions may influence active site configuration. One interpretation of the present results is that while the T4moH active site provides an overall preference for *p*-cresol formation in the absence of T4moD, binding interactions mediated by T4moD give rise to an incremental adjustment of the active site residues that ultimately yield the highest regiospecificity. The relaxation of regiospecificity observed in the mutated T4moH isoforms, accentuated in the absence of T4moD, may then reflect the presence of several unique, energetically equivalent binding conformations in an incompletely organized active site. Since T4moD binding increases the rate of catalysis, complex formation may also restrict substrate rotational and translational motion during the lifetime of oxidizing intermediates and contribute to the observed results. Furthermore, the strength of the electrophile is known to play a significant role in determining the product distribution in electrophilic aromatic substitution reactions. Since no T4moH isoform was able to oxidize nitrobenzene in the absence of T4moD, it is possible that the reactivity of the enzyme electrophile may be modulated by complex formation in the T4MO system. This result is distinct from that obtained with MMO, where all substrates that were oxidized by the MmoH−MmoB complex, including nitrobenzene, were also oxidized by MmoH lacking MmoB (*20*). This putative change in the oxidative capability of T4moH may also contribute to the increased fraction of *ortho* products from the *ortho/para* directing substrates.

Use of Mutagenesis in Studies of Diiron Hydroxylases. The X-ray structures of MmoH (*61*, *74*−*77*) and the NMR structures of P2 (*78*), MmoB (*79*−*82*), and T4moD (*44*) have provided an effective basis for analyzing primary sequence alignments and for inferring structural relationships between the different members of the diiron hydroxylase family.

These structures have also served as the starting point for mutagenesis efforts such as those described here and elsewhere (*34*, *45*, *46*).

The apparent V_{max}/K_M specificities of the T4moH isoforms studied here for reaction with toluene differed by only ~2−4-fold, while the coupling efficiencies ranged from 81% to 98% (Table 4). Within the set of aromatic substrates examined, the apparent V_{max} values differed by ~30-fold and could be approximately correlated with the electronic properties of the substrates (Table 3). Steady-state V_{max} values and coupling efficiencies were not obligately linked, as the T201 isoform gave an ~4-fold slower turnover rate for the oxidation of benzene as compared to toluene with the same coupling efficiency for both substrates (Table 3), while the T201G isoform gave a higher turnover rate for toluene oxidation as compared to the T201 isoform, albeit with slightly decreased coupling. These results suggest that once electrons are transferred from T4moC into the T4moD−T4moH complex, the remaining aspects of the catalytic cycle have overall comparable function and performance with respect to O_2-activation chemistry and toluene hydroxylation in each of the various isoforms studied.

Lowered coupling efficiency was observed for the nonnatural substrates. The uncoupling observed for nitrobenzene and cyclohexane may arise either from the inherent challenge of reaction with a chemically difficult to oxidize substrate based on electronic considerations or from the misalignment of a nonaromatic, nonplanar substrate in the active site, respectively. Previous studies of cytochrome P450 enzymes have indicated that increased access of solvent (*83*), altered patterns of proton transfer (*84*, *85*), release of H_2O_2 (*86*), or the reduction of stalled activated intermediates by subsequent electron-transfer reactions can also lead to uncoupling. For the diiron enzymes, each of these aspects is also possible and, in principle, may be influenced by conformational changes provided by protein−protein interactions. Among other effects, MmoB binding has been proposed to limit H_2O_2 release from compound P-level intermediates (*34*), while a rapid electron transfer to an activated intermediate is an essential feature of the physiological reactivity of ribonucleotide reductase R2 component (*87*−*89*) and the NADH peroxidase activity identified for MmoH from *Methylococcus capsulatus* (Bath) (*42*).

Figure 6 shows that regiospecificity is substantially influenced by steric interactions in the enzyme active site, with an ~100-fold difference in the *para*/*ortho* ratio given by the complete T4MO complex as compared to the product distributions given either by the T4MO complex lacking T4moD or by solution-based oxidations [nitration (*90*) or H_2O_2- and $AgCl_2$-catalyzed hydroxylation (*91*)]. In the absence of T4moD, the *para/ortho* ratios shifted, suggesting that one role of the T4moD−T4moH complex is to maintain (or produce) the proper steric orientation between the substrate and the diiron oxidant. Upon consideration of the changes in regiospecificity observed from the various T4moH isoforms both with and without T4moD (or T3buV), these binding interactions must produce a conformational change in the substrate binding site, regardless of the identity of the amino acids provided in the enzyme active site by the T4moH isoform.

The reactivity of the G103L isoform of T4moH with all substrates tested shows that this isoform can be favorably compared to the natural isoform with respect to V_{max}, V_{max}/K_M, and coupling efficiency (Tables 3 and 4). These comparisons indicate that interactions with the other protein components as well as the details of the catalytic cycle attributable to the diiron center are essentially unaltered in this minimally engineered isoform. However, for each substrate examined, the regiospecificity of hydroxylation given by the G103L isoform was significantly different from that of the natural isoform. These results indicate that a single amino acid change can potentially lead to the creation of a catalytically distinct and physiologically relevant diiron hydroxylase variant.

With the exception of nitrobenzene, the regiospecificity of the G103L isoform was substantially shifted toward *ortho* hydroxylation in the presence of T4moD. This tendency was enhanced by removal of T4moD from the catalytic complex, albeit with the losses in catalytic rate and coupling associated with complex formation. For chlorobenzene a large increase in the amount of the *meta*-hydroxylation product was observed with the G103L isoform. Previous studies of the reactions of synthetic chlorobenzene epoxides showed that *meta*-hydroxylation products were not observed from the decomposition of synthetic chlorobenzene 2,3- or 3,4-epoxides (*92*). Furthermore, the lifetime of these chlorobenzene epoxides in aqueous solution is relatively long (*93*), suggesting that a putative enzymic chlorobenzene epoxide product could readily difuse from the T4moH active site during steady-state turnover. Since the product distributions observed from chlorobenzene with the G103L isoform clearly deviate from the results of the chemical decomposition experiments, these results further support the role of the T4moH active site in orienting the substrate for hydroxylation, in selectively promoting the rapid decomposition of an enzyme-bound epoxide, or perhaps both.

Biological Imperative for Regio- or Stereospecificity in Diiron Hydroxylases. In methanotrophic bacteria, methane is the only physiologically relevant substrate for MMO as adventitious oxidations of other substrates do not provide a sole source of carbon or energy.[3] Since methane and methanol are achiral, no unique stereochemical imperative can be attributed to the biological function of MmoH.

In the alkene monooxygenase reactions, a 92−95% excess of the (*R)*-epoxypropane enantiomer has been observed from reaction with propene (*15*). The degree to which this enantiomeric excess is promoted by effector protein binding has not been reported. However, as with T4moH, it is likely that both the interior surface of the alkene monooxygenase active site and effector protein binding will contribute substantially to the fidelity of this reaction. Propene-utilizing microorganisms consume both epoxide enantiomers arising from the alkene monooxygenase reaction due to the coordinate induction of isoformic dehydrogenases with stereoselectivity for the 2(*R*)- and 2(*S*)-hydroxypropyl-CoM prod-

[3] In special cases, adventitious oxidations give products that can be utilized for growth by methanotrophs (*1*). For example, adventitious hydroxylation of chloromethane yields formaldehyde upon nonenzymatic elimination of chloride from a putative chlorohydrin intermediate. However, this nonenzymatic elimination reaction bypasses a key oxidation step required for electron transport and energy conservation in methanotrophs, the methanol dehydrogenase-catalyzed oxidation of methanol to formaldehyde. Hence, chloromethane does not serve as a growth substrate.

ucts of epoxyalkane:coenzyme M transferase (*94*). Thus a substantial cellular commitment is required to account for the minor fraction of a potentially toxic product derived from relaxed regiospecificity.

Bacteria containing the natural isoforms of the diiron toluene/benzene hydroxylases with regiospecificity for *ortho* (*13*), *meta* (*10*, *48*), and *para* (*45*) hydroxylation of toluene have been reported. In *Pseudomonas mendocina* KR1, the organism from which T4MO was obtained, the biological imperative for *para* hydroxylation is enforced by the next step in the metabolic pathway, where *p*-cresol methyl hydroxylase must form a quinone methide intermediate from *p*-cresol in order to complete the water-derived hydroxylation reaction (*95*). Consequently, *o*- and *m*-cresols cannot be utilized by *P. mendocina* KR1 (*96*−*98*), and their formation would thus represent a waste of energy and competitive disadvantage to the cell. Furthermore, in pure culture, these products of a low-specificity monooxygenation accumulate as toxic metabolites. In contrast to *P. mendocina* KR1, the majority of the organisms in the toluene/benzene hydroxylase family are capable of using all three cresol isoforms as growth substrates. These organisms convert the cresol isomers into methyl-substituted catechols that are subsequently metabolized by the extradiol cleavage pathway (*99*−*103*). The extradiol pathway has long been recognized for tolerance to the position of methyl and other substituents on the aromatic ring (*104*), thus providing the necessary enzymatic versatility to cope with the low regiospecificity of initial monooxygenase reactions.

Comparison with Other Toluene Monooxygenase Complexes. The toluene 2-monooxygenase from *B. cepacia* G4 has been purified and shown to hydroxylate toluene to give *o*-cresol and to also hydroxylate *o*-cresol to give 3-methylcatechol (*7*). This pattern of reactivity and the lack of catalytic complementation when the S1 effector protein was used to reconstitute T4MO provide functional support for our assignment of the *B. cepacia* G4 enzyme to the phenol hydroxylase branch of the diiron hydroxylase family tree (*44*). In the toluene hydroxylation reaction, the purified G103L isoform of T4moH has a turnover number ~20-fold higher (1.8 s^{-1}, Table 3) than that reported for the purified *B. cepacia* G4 enzyme [0.09 s^{-1} (*7*)]. However, unlike the more rapid oxidation of 2-methylphenol catalyzed by the *B. cepacia* G4 enzyme [0.46 s^{-1} (*7*)], the G103L isoform does not oxidize *p*-cresol to yield a catecholic product. Since the *B. cepacia* G4 enzyme has a Leu residue at the same sequence position as the G103L isoform of T4moH, other, presently unknown, active site features must give rise to differences in the primary substrate selectivities observed for the toluene/benzene and phenol hydroxylase branches of the diiron hydroxylase phylogenetic tree (*44*).

The product distribution given by G103L from toluene (Figure 2) is comparable to that observed in other naturally occurring members of the toluene/benzene hydroxylase branch of the diiron hydroxylase phylogenetic tree (*12*, *13*, *48*). Thus the enzyme cloned from *Pseudomonas aeruginosa* JI104 (*12*) converted toluene to a mixture of *o*-cresol (21%), *m*-cresol (42%), and *p*-cresol (37%), while the enzyme from *Pseudomonas stutzeri* OX1 produced larger amounts of *o*-cresol (50%) than either *p*-cresol (31%) or *m*-cresol (19%) (percentages estimated from Figure 3 of ref *13*). In natural environments, a G103L isoform of T4moH could arise by transversion at two adjacent nucleotides, GGT → CTT, with the sequential conversion of Gly → Val → Leu corresponding to a plausible natural progression given by single nucleotide changes. In support of this route to evolutionary diversity, each of these amino acids is found in naturally occuring diiron hydroxylases. For example, alkene monooxygenase from *Xanthobacter* species Py2 has a Val residue at this position, while T2MO from *B. cepacia* G4 and *Pseudomonas* species JS150 and phenol hydroxylase from *Pseudomonas* species CF600 each have Leu residues at this position. In order for these mutations to give rise to a naturally occurring enzyme isoform, they would likely have to occur in the context of a host containing the requisite pathways for subsequent metabolism of the alternative cresol products, such as that present in *P. stutzeri* OX1 (*103*). The incorporation of the genes encoding these gene clusters and metabolic pathways on naturally transmissible plasmids could indeed facilitate the horizontal transfers required for this putative enzyme evolution process.

Relevance of T4moH Isoform G103L to Diiron Enzyme Reactivity. Primary sequence alignments (*57*, *59*) show that many, but not all, diiron hydroxylases have a Gly residue that aligns with G103 in T4moH. This position is adjacent to a conserved Glu residue that acts as an iron ligand to the canonical Fe_A site. In a related diiron enzyme, the R2 component of ribonucleotide reductase, D84 provides the corresponding iron ligand to Fe_A (*105*). Recent studies of an R2 isoform with a D84E mutation (and a distant W48F mutation that changes electron- transfer rates and stoichiometry) show that the introduced change in metal binding ligand produces a diferrous center configuration more closely matching that of diferrous MmoH. This structural change apparently imparts stability to a compound P-like intermediate and yields a more efficient self-hydroxylating monooxygenase reaction where the O atom incorporated has been demonstrated to arise from O_2 (*65*, *106*). Thus a slight change in structure can lead to profound changes in the outcome of the reaction. The catalytic results presented here correlate substantial alterations of substrate regiospecificity with changes in a nonligand amino acid at a position adjacent to the comparable Fe_A iron ligand of a diiron hydroxylase. Further examination of this region as an important locus of chemical reactivity within the diiron enzyme active site thus seems warranted.

REFERENCES

1. Anthony, C. (1982) in *The Biochemistry of Methylotrophs*, p 431, Academic Press, New York.
2. Green, J., and Dalton, H. (1985) *J. Biol. Chem. 260*, 15795−15801.
3. Patel, R. N., and Savas, J. C. (1987) *J. Bacteriol. 169*, 2313−2317.
4. Fox, B. G., Froland, W. A., Dege, J. E., and Lipscomb, J. D. (1989) *J. Biol. Chem. 264*, 10023−10033.
5. Shen, R., Yu, C., Ma, Q., and Li, S. (1997) *Arch. Biochem. Biophys. 345*, 223−229.
6. Grosse, S., Laramee, L., Wendlandt, K. D., McDonald, I. R., Miguez, C. B., and Kleber, H. P. (1999) *Appl. Environ. Microbiol. 65*, 3929−3935.
7. Newman, L. M., and Wackett, L. P. (1995) *Biochemistry 34*, 14066−14076.
8. Johnson, G. R., and Olsen, R. H. (1995) *Appl. Environ. Microbiol. 61*, 3336−3346.

9. Pikus, J. D., Studts, J. M., Achim, C., Kauffmann, K. E., Münck, E., Steffan, R. J., McClay, K., and Fox, B. G. (1996) *Biochemistry 35*, 9106−9119.
10. Byrne, A. M., Kukor, J. J., and Olsen, R. H. (1995) *Gene 154*, 65−70.
11. Studts, J. M., Mitchell, K. H., Pikus, J. D., McClay, K., Steffan, R. J., and Fox, B. G. (2000) *Protein Expression Purif. 20*, 58−65.
12. Kitayama, A., Suzuki, E., Kawakami, Y., and Nagamune, T. (1996) *J. Ferment. Bioeng. 82*, 421−425.
13. Bertoni, G., Bolognese, F., Galli, E., and Barbieri, P. (1996) *J. Bacteriol. 62*, 3704−3711.
14. Powlowski, J., and Shingler, V. (1990) *J. Bacteriol. 172*, 6834−6840.
15. Small, F. J., and Ensign, S. A. (1997) *J. Biol. Chem. 272*, 24913−24920.
16. Miura, A., and Dalton, H. (1995) *Biosci. Biotechnol. Biochem. 59*, 853−859.
17. Zhou, N. Y., Jenkins, A., Chan Kwo Chion, C. K., and Leak, D. J. (1999) *Appl. Environ. Microbiol. 65*, 1589−1595.
18. Smith, T. J., Lloyd, J. S., Gallagher, S. C., Fosdike, W. L., Murrell, J. C., and Dalton, H. (1999) *Eur. J. Biochem. 260*, 446−452.
19. Andersson, K. K., Froland, W. A., Lee, S.-K., and Lipscomb, J. D. (1991) *New J. Chem. 15*, 411−415.
20. Froland, W. A., Andersson, K. K., Lee, S.-K., Liu, Y., and Lipscomb, J. D. (1992) *J. Biol. Chem. 267*, 17588−17597.
21. Jiang, Y., Wilkins, P. C., and Dalton, H. (1993) *Biochim. Biophys. Acta 1163*, 105−112.
22. Lee, S.-K., Nesheim, J. C., and Lipscomb, J. D. (1993) *J. Biol. Chem. 268*, 21569−21577.
23. Lee, S.-K., Fox, B. G., Froland, W. F., Lipscomb, J. D., and Münck, E. (1993) *J. Am. Chem. Soc. 115*, 6450−6451.
24. Liu, K. E., Valentine, A. M., Qui, D., Edmondson, D. E., Appelman, E. H., Spiro, T. G., and Lippard, S. J. (1995) *J. Am. Chem. Soc. 117*, 4997−4998.
25. Liu, K. E., Valentine, A. M., Wang, D., Huynh, B. H., Edmondson, D. E., Salifoglou, A., and Lippard, S. J. (1995) *J. Am. Chem. Soc. 117*, 10174−10185.
26. Shu, L., Nesheim, J. C., Kauffmann, K., Münck, E., Lipscomb, J. D., and Que, L., Jr. (1997) *Science 275*, 515−518.
27. Liu, K. E., Valentine, A. M., Qui, D., Edmondson, D. E., Appelman, E. H., Spiro, T. G., and Lippard, S. J. (1997) *J. Am. Chem. Soc. 119*, 11134−11136.
28. Valentine, A. M., Tavares, P., Pereira, A. S., Davydov, R., Krebs, C., Hoffman, B. M., Edmondson, D. E., Huynh, B. H., and Lippard, S. J. (1998) *J. Am. Chem. Soc. 120*, 2190−2191.
29. Lee, S.-K., and Lipscomb, J. D. (1999) *Biochemistry 38*, 4423−4432.
30. Valentine, A. M., Stahl, S. S., and Lippard, S. J. (1999) *J. Am. Chem. Soc. 121*, 3867−3887.
31. Brazeau, B. J., and Lipscomb, J. D. (2000) *Biochemistry 39*, 13503−13515.
32. Brazeau, B. J., and Lipscomb, J. D. (2000) *Subcell. Biochem. 35*, 233−277.
33. Stahl, S. S., Francisco, W. A., Merkx, M., Klinman, J. P., and Lippard, S. J. (2001) *J. Biol. Chem. 276*, 4549−4553.
34. Wallar, B. J., and Lipscomb, J. D. (2001) *Biochemistry 40*, 2220−2233.
35. Brazeau, B., Austin, R., Groves, J. T., and Lipscomb, J. D. (2001) *J. Am. Chem. Soc.* (in press).
36. Fox, B. G., Liu, Y., Dege, J. E., and Lipscomb, J. D. (1991) *J. Biol. Chem. 266*, 540−550.
37. Gallagher, S. C., Callaghan, A. J., Zhao, J., Dalton, H., and Trewhella, J. (1999) *Biochemistry 38*, 6752−6760.
38. Paulsen, K. E., Liu, Y., Fox, B. G., Lipscomb, J. D., Münck, E., and Stankovich, M. T. (1994) *Biochemistry 33*, 713−722.
39. Pulver, S., Froland, W. A., Fox, B. G., Lipscomb, J. D., and Solomon, E. I. (1993) *J. Am. Chem. Soc. 115*, 12409−12422.
40. Liu, Y., Nesheim, J. C., Lee, S.-K., and Lipscomb, J. D. (1995) *J. Biol. Chem. 270*, 24662−24665.
41. Liu, Y., Nesheim, J. C., Paulsen, K. E., Stankovich, M. T., and Lipscomb, J. D. (1997) *Biochemistry 36*, 5223−5233.
42. Gassner, G. T., and Lippard, S. J. (1999) *Biochemistry 38*, 12768−12785.
43. Scognamiglio, R., Notomista, E., Barbieri, P., Pucci, P., Dal Piaz, F., Tramontano, A., and Di Donato, A. (2001) *Protein Sci. 10*, 482−490.
44. Hemmi, H., Studts, J. M., Chae, Y. K., Song, J., Markley, J. L., and Fox, B. G. (2001) *Biochemistry 40*, 3512−3524.
45. Pikus, J. D., Studts, J. M., McClay, K., Steffan, R. J., and Fox, B. G. (1997) *Biochemistry 36*, 9283−9289.
46. Pikus, J. D., Mitchell, K. H., Studts, J. M., McClay, K., Steffan, R. J., and Fox, B. G. (2000) *Biochemistry 39*, 791−799.
47. Oppenheim, S. F., Studts, J. M., Fox, B. G., and Dordick, J. S. (2001) *Appl. Biochem. Biotechnol. 90*, 187−197.
48. Olsen, R. H., Kukor, J. J., and Kaphammer, B. (1994) *J. Bacteriol. 176*, 3749−3756.
49. Chenault, H. K., and Whitesides, G. M. (1987) *Appl. Biochem. Biotechol. 14*, 147−197.
50. Haas, J. A., and Fox, B. G. (1999) *Biochemistry 38*, 12833−12840.
51. Cleland, W. W. (1979) *Methods Enzymol. 63*, 103−139.
52. Fox, B. G., Borneman, J. G., Wackett, L. P., and Lipscomb, J. D. (1990) *Biochemistry 29*, 6419−6427.
53. Doidy, V., Carre, B., Bouchoule, C., Barrault, J., and Blanchard, M. (1995) *Bull. Soc. Chim. Belg. 104*, 431−437.
54. Taylor, R. (1990) in *Electrophilic Aromatic Substitution*, p 513, John Wiley & Sons, New York.
55. Park, S. J., and Gunsalus, R. P. (1995) *J. Bacteriol. 177*, 6255−6262.
56. Massey, V. (1980) *U. Mich. Med. Center J. 46*, 28−37.
57. Fox, B. G., Shanklin, J., Ai, J., Loehr, T. M., and Sanders-Loehr, J. (1994) *Biochemistry 33*, 12776−12786.
58. Fox, B. G. (1998) in *Comprehensive Biological Catalysis* (Sinnott, M., Ed.) pp 261−348, Academic Press, London.
59. Coufal, D. E., Blazyk, J., Whittington, D. A., Wu, W. W., Rosenzweig, A. C., and Lippard, S. J. (2000) *Eur. J. Biochem. 267*, 2174−2185.
60. Yen, K.-M., Karl, M. R., Blatt, L. M., Simon, M. J., Winter, R. B., Fausset, P. R., Lu, H. S., Harcourt, A. A., and Chen, K. K. (1991) *J. Bacteriol. 173*, 5315−5327.
61. Rosenzweig, A. C., Nordlund, P., Takahara, P. M., Frederick, C. A., and Lippard, S. J. (1995) *Chem. Biol. 2*, 409−418.
62. Atta, M., Nordlund, P., Åberg, A., Eklund, H., and Fontecave, M. (1992) *J. Biol. Chem. 267*, 20682−20688.
63. Åberg, A., Nordlund, P., and Eklund, H. (1993) *Nature 361*, 276−278.
64. Logan, D. T., Su, X.-D., Åberg, A., Regnström, K., Hajdu, J., Eklund, H., and Nordlund, P. (1996) *Structure 4*, 1053−1064.
65. Voegtli, W. C., Khidekel, N., Baldwin, J., Ley, B. A., Bollinger, J. M., Jr., and Rosenzweig, A. C. (2000) *J. Am. Chem. Soc. 122*, 3255−3261.
66. Pulver, S. C., Tong, W. H., Bollinger, J. M., Stubbe, J., and Solomon, E. I. (1995) *J. Am. Chem. Soc. 117*, 12664−12678.
67. Yang, Y.-S., Broadwater, J. A., Fox, B. G., and Solomon, E. I. (1999) *J. Am. Chem. Soc. 121*, 2770−2783.
68. Davydov, R., Valentine, A. M., Komar-Panicucci, S., Hoffman, B. M., and Lippard, S. J. (1999) *Biochemistry 38*, 4188−4197.
69. Willems, J.-P., Valentine, A. M., Gurbiel, R., Lippard, S. J., and Hoffman, B. M. (1998) *J. Am. Chem. Soc. 120*, 9410−9416.
70. Davydov, A., Davydov, R., Graslund, A., Lipscomb, J. D., and Andersson, K. K. (1997) *J. Biol. Chem. 272*, 7022−7026.
71. DeRose, V. J., Liu, K. E., Lippard, S. J., and Hoffman, B. M. (1996) *J. Am. Chem. Soc. 118*, 121−134.
72. Shu, L., Liu, Y., Lipscomb, J. D., and Que, L., Jr. (1996) *J. Biol. Inorg. Chem. 1*, 297−304.
73. Fox, B. G., Hendrich, M. P., Surerus, K. K., Andersson, K. K., Froland, W. A., Lipscomb, J. D., and Münck, E. (1993) *J. Am. Chem. Soc. 115*, 3688−3701.
74. Rosenzweig, A. C., Frederick, C. A., Lippard, S. J., and Nordlund, P. (1993) *Nature 336*, 537−543.
75. Rosenzweig, A. C., Brandstetter, H., Whittington, D. A., Nordlund, P., Lippard, S. J., and Frederick, C. A. (1997) *Proteins 29*, 141−152.

76. Whittington, D. A., Rosenzweig, A. C., Frederick, C. A., and Lippard, S. J. (2001) *Biochemistry 40*, 3476−3482.
77. Elango, N., Radhakrishnan, R., Froland, W. A., Wallar, B. J., Earhart, C. A., Lipscomb, J. D., and Ohlendorf, D. H. (1997) *Protein Sci. 6*, 556−568.
78. Qian, H., Edlund, U., Powlowski, J., Shingler, V., and Sethson, I. (1997) *Biochemistry 36*, 495−504.
79. Chang, S.-L., Wallar, B. J., Lipscomb, J. D., and Mayo, K. H. (1999) *Biochemistry 38*, 5799−5812.
80. Chang, S.-L., Wallar, B. J., Lipscomb, J. D., and Mayo, K. H. (2001) *Biochemistry 40*, 9539−9551.
81. Walters, K., Gassner, G. T., Lippard, S. J., and Wagner, G. (1999) *Proc. Natl. Acad. Sci. U.S.A. 96*, 7877−7882.
82. Matsuo, H., Walters, K. J., Teruya, K., Tanaka, T., Gassner, G. T., Lippard, S. J., Kyogoku, Y., and Wagner, G. (1999) *J. Am. Chem. Soc. 121*, 9903−9904.
83. Loida, P. J., and Sligar, S. G. (1993) *Biochemistry 32*, 11530−11538.
84. Gerber, N. C., and Sligar, S. G. (1992) *J. Am. Chem. Soc. 114*, 8742−8743.
85. Atkins, W. A., and Sligar, S. G. (1988) *J. Biol. Chem. 263*, 18842−18849.
86. Martinis, S. A., Atkins, W. A., Stayton, P. S., and Sligar, S. G. (1989) *J. Am. Chem. Soc. 111*, 9252−9253.
87. Bollinger, J. M., Jr., Tong, W. H., Ravi, N., Huynh, B. H., Edmondson, D. E., and Stubbe, J. (1994) *J. Am. Chem. Soc. 116*, 8015−8023.
88. Bollinger, J. M., Jr., Tong, W. H., Ravi, N., Huynh, B. H., Edmondson, D. E., and Stubbe, J. (1994) *J. Am. Chem. Soc. 116*, 8024−8032.
89. Parkin, S. E., Chen, S., Ley, B. A., Mangravite, L., Edmondson, D. E., Huynh, B. H., and Bollinger, J. M., Jr. (1998) *Biochemistry 37*, 1124−1130.
90. Carey, F. A., and Sundberg, R. J. (1990) in *Advanced Organic Chemistry*, Part A, Plenum Press, New York.
91. Kurz, M. E., and Johnson, G. J. (1971) *J. Org. Chem. 36*, 3184−3187.
92. Selander, H. G., Jerina, D. M., Piccolo, D. E., and Berchtold, G. A. (1975) *J. Am. Chem. Soc. 97*, 4428−4430.
93. Kasperek, G. J., Bruice, T. C., Yagi, H., and Jerina, D. M. (1972) *J. Chem. Soc., Chem. Commun*.
94. Allen, J. R., and Ensign, S. A. (1999) *Biochemistry 38*, 247−256.
95. Hopper, D. J. (1978) *Biochem. J. 175*, 345−347.
96. Whited, G. M., and Gibson, D. T. (1991) *J. Bacteriol. 173*, 3017−3020.
97. McClay, K., Streger, S. H., and Steffan, R. J. (1995) *Appl. Environ. Microbiol. 61*, 3479−3481.
98. McClay, K., Fox, B. G., and Steffan, R. J. (1996) *Appl. Environ. Microbiol. 62*, 2716−2722.
99. Byrne, A. M., and Olsen, R. H. (1996) *J. Bacteriol. 178*, 6327−6337.
100. Johnson, G. R., and Olsen, R. H. (1997) *Appl. Environ. Microbiol. 63*, 4047−4052.
101. Leahy, J. G., Johnson, G. R., and Olsen, R. H. (1997) *Appl. Environ. Microbiol. 63*, 3736−3739.
102. Powlowski, J., and Shingler, V. (1994) *Biodegradation 5*, 219−236.
103. Arenghi, F. L., Berlanda, D., Galli, E., Sello, G., and Barbieri, P. (2001) *Appl. Environ. Microbiol. 67*, 3304−3308.
104. Dagley, S. (1984) *Dev. Ind. Microbiol. 25*, 53−65.
105. Nordlund, P., and Eklund, H. (1993) *J. Mol. Biol. 232*, 123−164.
106. Baldwin, J., Voegtli, W. C., Khidekel, N., Moënne-Loccoz, P., Krebs, C., Pereira, A. S., Ley, B. A., Huynh, B. H., Loehr, T. M., Riggs-Gelasco, P. J., Rosenzweig, A. C., and Bollinger, J. M., Jr. (2001) *J. Am. Chem. Soc. 123*, 7017−7030.

BI012036P